Torsional responses of double-walled carbon nanotubes via molecular dynamics simulations

2008 J. Phys.: Condens. Matter 20 455214

(http://iopscience.iop.org/0953-8984/20/45/455214)

IOP PUBLISHING JOURNAL OF PHYSICS: CONDENSED MATTER
J. Phys.: Condens. Matter **20** (2008) 455214 (6pp) doi:10.1088/0953-8984/20/45/455214

Torsional responses of double-walled carbon nanotubes via molecular dynamics simulations

Y Y Zhang and C M Wang[1]

Engineering Science Programme and Department of Civil Engineering, National University of Singapore, Kent Ridge, 119260, Singapore

E-mail: cvewcm@nus.edu.sg

Received 4 August 2008, in final form 17 September 2008
Published 13 October 2008
Online at stacks.iop.org/JPhysCM/20/455214

Abstract
The buckling behaviors of double-walled carbon nanotubes (DWCNTs) under torsion are investigated by using molecular dynamics (MD) simulations. The effect of length on the torsional buckling behaviors of DWCNTs is examined for the first time. The simulation results show that the DWCNTs experience gradual or simultaneous buckling deformations depending on their lengths. In addition, the effect of the inner tube in a DWCNT on its torsional buckling behavior is also examined. The presence of the inner tube triggers van der Waals (vdW) interactions between it and the outer tube and thus leads to a stiffening effect of the DWCNT against torsional deformation. Whether the ends of the inner tube are free or fixed and whether it is subject to a torque or not, the critical torque and the critical torsional angle of the outer tube are only marginally affected.

(Some figures in this article are in colour only in the electronic version)

1. Introduction

Intensive experimental and theoretical studies on carbon nanotubes (CNTs) have been carried out by researchers worldwide to characterize their remarkable properties, to develop mathematical models, to analyze and even to design nanostructures using these CNTs. So far, CNTs have shown great potential applications as components in nanoelectromechanical systems (NEMS) such as actuators [1], springs [2] and oscillators [3]. In such applications, it is crucial to know the mechanical properties and to understand their behavior when subject to forces and moments.

When compared to the intensive studies devoted to buckling analysis and behaviors of CNTs under axial compression [4–13] or bending [14–19], relatively few investigations have been carried out on the torsional behavior of CNTs. Based on Brenner's potential [20], Yakobson *et al* [21] carried out MD simulations on an armchair single-walled CNT (SWCNT) under axial compression, bending and torsion and compared the solutions with those obtained by a thin cylindrical shell model. They observed that the continuum shell model could predict the buckling behaviors of SWCNTs satisfactorily provided that the mechanical parameters such as the Young modulus and the effective wall thickness are judiciously adopted. Inspired by this pioneering work, various thin shell models have been proposed and widely applied in the buckling analysis of CNTs subject to axial compressive loading as well as torsional loading. Han and Lu [22] applied a multiple shell model, developed by Ru [23], to analyze the torsional buckling behavior of a double-walled CNT (DWCNT) embedded in an elastic medium. Later, Yao and Han [24] considered the temperature change in the multiple shell model so as to investigate the effect of temperature change on the torsional buckling modes and critical torques of multi-walled CNTs (MWCNTs). Recently, Wang *et al* [25] proposed the Kromm shell model for the torsional buckling analysis of short or moderately long SWCNTs. In addition to the continuum mechanics analyses, some MD simulations have also been performed to analyze the geometrical effects on the torsional characteristics of SWCNTs and MWCNTs. Wang *et al* [26] showed that the shear modulus of a zigzag SWCNT is higher than that of its armchair counterpart. Moreover, the

[1] Author to whom any correspondence should be addressed.

shear modulus increases as the radius of the SWCNT increases. Chang [27] investigated SWCNTs with chiral angles ranging from 0° to 30° under torsion and found that the critical torsional strain of the SWCNTs is dependent on the loading direction because of its structural asymmetry. Jeong [28] characterized the torsional properties of different CNT systems such as filled CNTs (CNTs filled with hydrogen atoms or nickel atoms), functionalized CNTs and CNT bundles. MD simulations carried out reveal that the critical torque can be enhanced by the presence of filling materials and having inner CNTs. The magnitude of this increase in critical torque depends on the types of filling materials and the number of inner tubes. Recently, Jeong *et al* [29] analyzed the effects of initial tensile stress or compressive stress on the torsional responses of CNTs and found that the presence of the initial stress affects the critical torque and torsional stiffness significantly. Williams *et al* [30] and Hall *et al* [31] carried out experiments on MWCNTs and SWCNTs, respectively, under torsion, with the view of obtaining their torsional properties. It is found from the literature search that few works have been done on the instability of CNTs under torsion, especially for MWCNTs because of their relatively complex structure. More studies are therefore required to characterize the torsional properties of MWCNTs before they can be employed as torsional springs in nanometer scale mechanical devices.

Complementing the earlier studies on CNTs under torsion, the present study will investigate the torsional behavior of DWCNTs. The study will make use of extensive MD simulations to compute the critical torsional angles and the torsional buckling modes of DWCNTs with different lengths, so as to explore the length effect on the torsional buckling behaviors of DWCNTs. It will be shown herein that the critical torque and the torsional buckling mode are significantly affected by the length of the DWCNT. In addition, the effect of the inner tube in a DWCNT is also considered.

2. Computational model

In the MD simulations, the bonding and non-bonding atomic interactions in a DWCNT are expressed by the widely used second-generation reactive empirical bond order (REBO) potential [32] and the Lennard-Jones (LJ) 12-6 potential [33], respectively. The initial energy-optimized configurations of the DWCNT are obtained by the conjugate gradient minimization method. The fifth-order Gear's predictor–corrector integration scheme is adopted with a time step size of 1 fs when integrating the equations of motion. The environmental temperature of the simulations is maintained at 0.01 K by a Berendsen thermostat [34]. The low temperature is chosen so as to avoid the thermal kinetic effect. Keeping the bottom ring of atoms fixed in position, the torsion of CNTs is achieved by rotating the top ring of atoms of both inner and outer tubes about the tube axis at a constant increment of the twisting angle. After each rotation increment of 1°, the entire DWCNT is fully relaxed for a certain time while restraining the top and bottom rings of atoms. The total torque applied to the DWCNT can be obtained by summing the product of the tangential force on each rotated atom and the respective radial distance of the atom from the tube axis. In the following sections, the simulation results of DWCNTs with different lengths are presented so as to examine the effect of length on the torsional properties of DWCNTs.

3. Length effect on torsional buckling behavior of DWCNTs

A set of (5, 5)/(10, 10) DWCNTs with lengths ranging from 41 to 213 Å is simulated to investigate the effect of tube length on the torsional buckling behavior of DWCNTs. In the simulations, five rings of atoms at the top ends of the inner and outer tubes are rotated at a constant twisting angle of 1° simultaneously. The whole DWCNT then moves freely except for the five rings of atoms at both ends. These boundary conditions are equivalent to clamped–clamped end conditions in an engineering mechanics analysis.

The simulation results show that the curves of the resultant torque and the strain energy against torsional angles are similar before buckling for all the DWCNTs. Here, we present the variations of the strain energy and torque curves with respect to the torsional angle of a 114.5 Å-long DWCNT in figures 1(a) and (b) as an illustration. The first regimes of the plots in figures 1(a) and (b) correspond to the almost homogeneous torsion of the tubes prior to the buckling, in which the strain energy follows closely a quadratic function of the torsional angle in accordance with Hooke's law. It can be seen that the resultant torque acting on the CNTs increases approximately linearly with respect to the torsional angle, as shown in figure 1(b). The outer tube buckles at the torsional angle of 100° followed by the inner one at 104°. The highest torques that the inner and outer tubes can withstand are 5.563 and 41.968 nN nm, respectively. The 114.5 Å-long DWCNT experiences a gradual twisting deformation which is dependent on the length, and this observation will be addressed in detail in the subsequent section.

The difference between the mechanical properties of SWCNTs and DWCNTs lies in the presence of van der Waals (vdW) interaction between the inner and outer tubes of the DWCNT. It is well known that the vdW interaction enhances the critical buckling strain of DWCNTs under axial compression [6, 35]. In order to assess the effect of vdW interaction on the torsional properties of DWCNTs, an individual 114.5 Å-long (10, 10) SWCNT is simulated under the identical simulation conditions. The SWCNT buckles at the critical torsional angle of 78° when subject to a torque of 31.848 nN nm. The critical torsional angle and the torque are significantly lower than 100° and 41.968 nN nm found for its corresponding DWCNT. It is clearly shown that the presence of the inner (5, 5) SWCNT in the (10, 10) SWCNT leads to a 22% increase in the critical torsional angle and a 24% increase in the critical torque. The inclusion of one CNT into another larger CNT can improve the torsional properties of the CNTs considerably due to the stiffening effect of vdW interactions

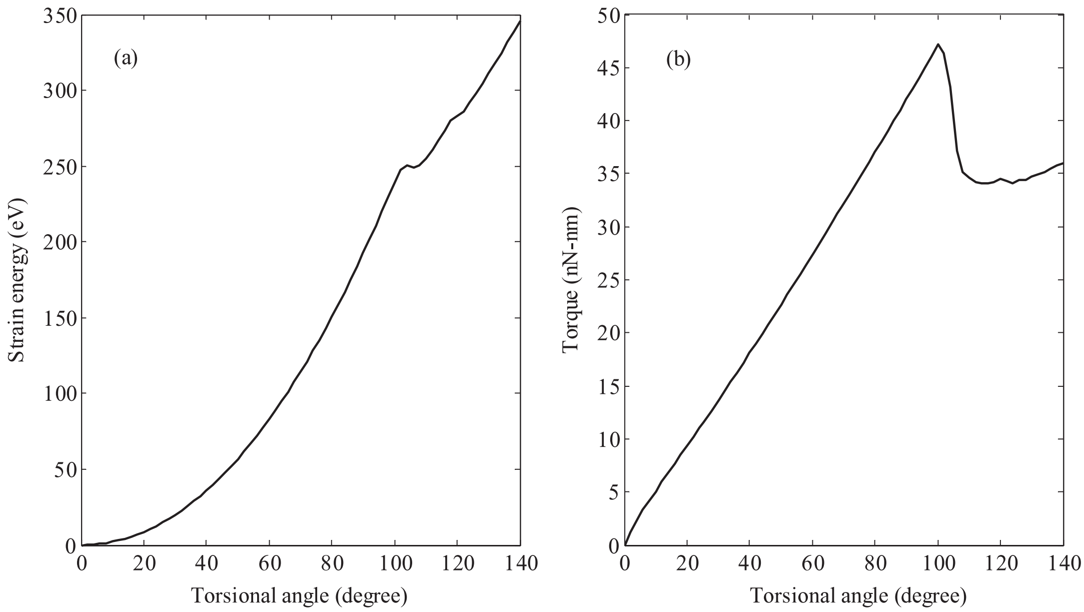

Figure 1. Variation of strain energy and torque with respect to torsional angle for DWCNTs.

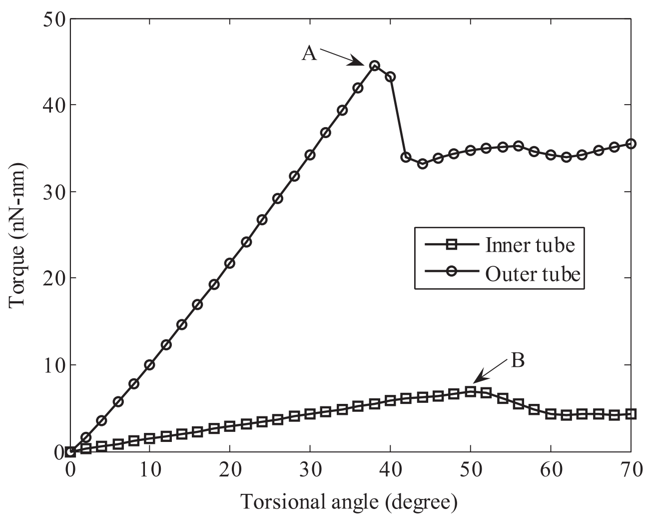

Figure 2. Relationship between torsional angle and torque in inner and outer tubes of a 40.6 Å-long DWCNT (points A and B indicate the highest torques).

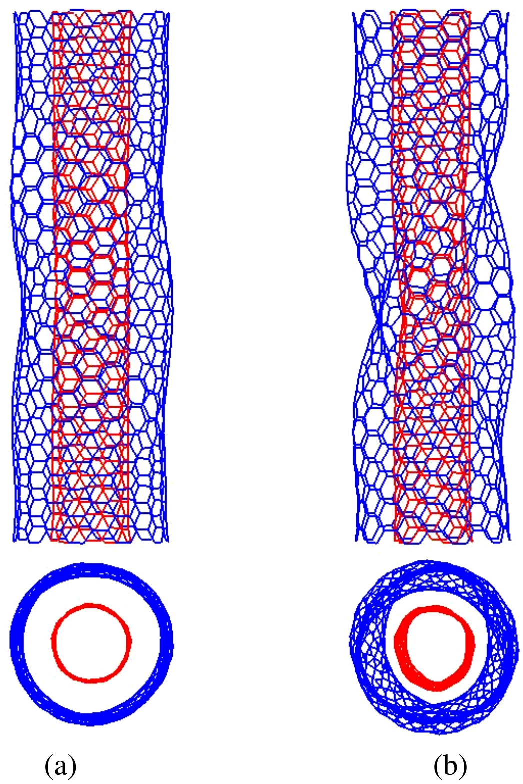

Figure 3. Torsional buckling modes of a 40.6 Å-long DWCNT: (a) outer tube buckles at torsional angle of 38° corresponding to point A in figure 2; (b) inner tube buckles at torsional angle of 50° corresponding to point B.

between the constituent CNTs. This observation also implies that MWCNTs are better candidates than SWCNTs as torsional springs in NEMS.

DWCNTs with lengths ranging from 41 to 213 Å were investigated to predict their individual mechanical response to torsion. Two different torsional buckling modes are observed, i.e. gradual and simultaneous modes. For relatively short DWCNTs, the outer tube reaches the highest torque first followed by the inner one under the same torsional angle, demonstrating a gradual buckling deformation as shown in figures 2 and 3. Figure 2 depicts the relationship between the torsional angles and the torque of the inner and outer tubes. Before buckling, the DWCNT undergoes homogeneous torsional deformation. Both torques acting on the inner and outer tubes increase linearly with respect to the torsional angles, as shown in figure 2. Owing to the larger diameter, the outer tube sustains a higher torque for the same torsional angle than its inner counterpart. In other words, the torsional stiffness

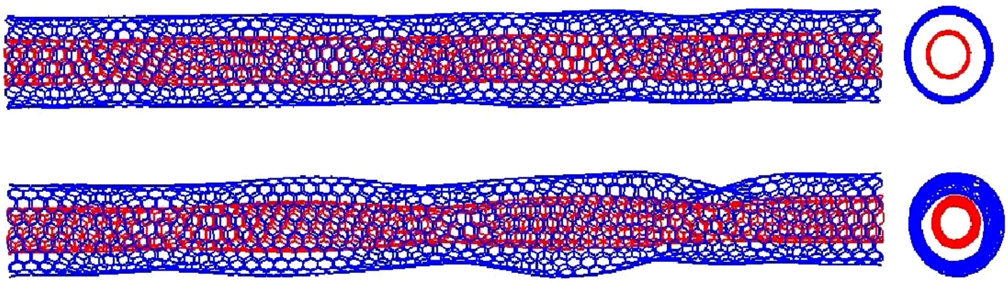

Figure 4. Gradual torsional buckling mode of a moderate long DWCNTs: (a) outer tube buckles followed by (b) the inner tube.

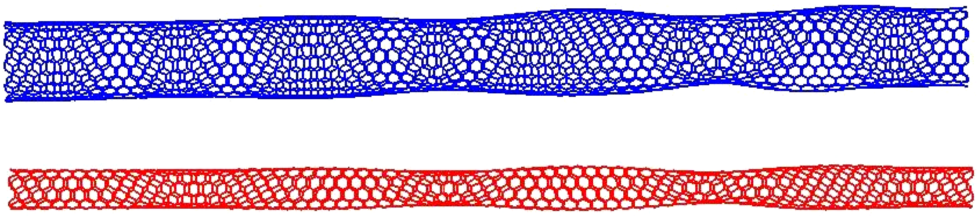

Figure 5. Torsional buckling mode of a slender DWCNT: (a) outer tube; (b) inner tube.

per unit length (the slope of the torque–torsional angle curve) of the outer tube is higher than that of the inner tube since the stiffness is varied as $K \sim D^3$ according to the continuum mechanics theory, where D is the diameter. However, the outer tube reaches the highest torque first at a torsional angle of 38° (point A in figure 2), indicating the occurrence of buckling. With further twisting of the DWCNT, the torque acting on the outer tube decreases significantly whereas the torque on the inner tube keeps increasing linearly until its critical torsional angle 50° is reached, as shown in figure 2 (point B). Points A and B in figure 2 denote the highest torques acting on the outer and inner tubes, respectively. The buckling modes of the DWCNT corresponding to points A and B in figure 2 are shown in figures 3(a) and (b). It is readily seen from figure 3(a) that the inner tube remains in the straight cylindrical geometry with a circular cross section when the outer tube buckles, thereby indicating that the inner tube is still stable. The torsional response of the inner and outer tubes is similar to a macroscopic hollow cylindrical shell. At the critical torsional angle of 38°, the outer tube buckles into a screw twisted thin shell with a corrugated appearance. When the inner tube reaches its critical torque, it also deforms as a twisted thin shell as shown in figure 3(b), but the distortion is less severe than that of the outer tube because the outer tube is subject to a higher shear strain level. The simulation results on other DWCNTs with different lengths are presented in table 1. DWCNTs with lengths up to 139.15 Å experience gradual buckling deformation with the outer tube buckling first followed by the inner one as shown in table 1 and figure 4. Although the moderately long DWCNTs undergo gradual buckling deformation, the deformation as shown in figure 4 resembles a twisted beam rather than a twisted shell shown in figure 3 for short DWCNTs. From table 1, it can be readily seen that the difference in the critical torsional angles between the inner and outer tubes depends strongly on the tube length.

Table 1. Simulation results of DWCNTs of various lengths.

	Critical torsional angle (deg)	
Length of DWCNTs (Å)	Inner tube	Outer tube
40.61	50	38
65.27	70	60
89.88	88	80
114.50	104	100
139.15	122	118
163.70	138	138
188.36	155	155
212.78	170	170

For short DWCNTs, the difference is larger while it is smaller for slender DWCNTs. The gradual buckling modes have also been reported by Wang [36] who performed MD simulations on (5, 0)/(14, 0) DWCNTs of length up to 100 Å. It should be pointed out that the DWCNTs simulated by Wang [36] are relatively short. Therefore, no simultaneous buckling mode was observed.

When the length of the DWCNTs is increasing, a simultaneous buckling mode is observed. The inner and outer tubes in the slender DWCNTs reach their critical torques almost simultaneously, and hence they buckle together into a screw twisted beam as shown in figure 5. In figure 5, the buckling morphologies of the outer and inner tubes are demonstrated individually so as to get a better view of the deformations. From figure 5, it can be seen that at the same critical torsional angle, the inner and outer tubes exhibit similar buckling modes. Additional simulations are performed on longer DWCNTs up to 212.78 Å and the results confirm the similar observations that are shown in figure 5.

From the intensive simulations on DWCNTs of various lengths, it is clear that there exist two different torsional

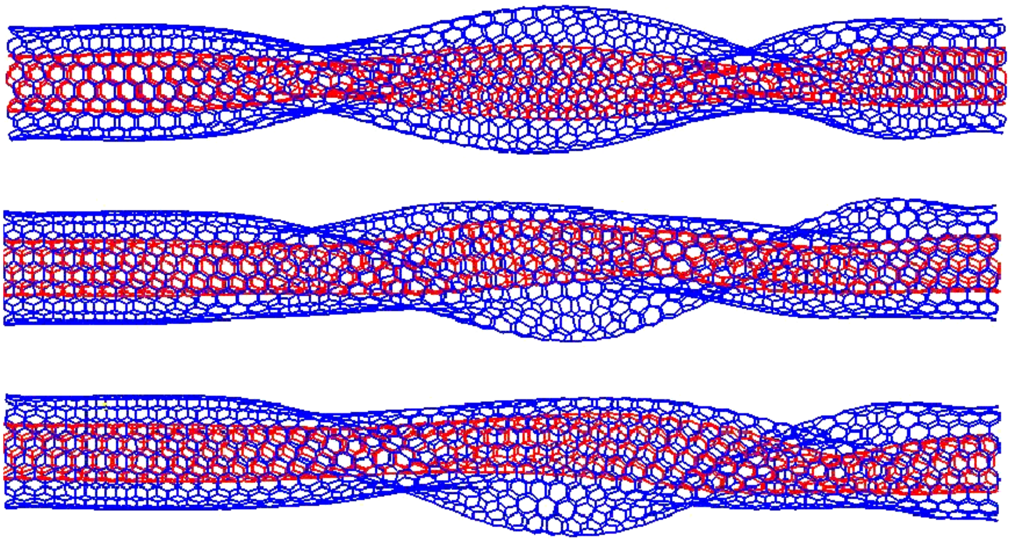

Figure 6. Post-buckling modes of DWCNTs under three different simulation conditions: (a) both outer and inner tubes subject to torque; (b) outer tube subject to torque only while inner tube is fixed at both ends; (c) outer tube subject to torque while the inner tube is totally free.

buckling modes, i.e. gradual and simultaneous buckling modes, depending on the length of the DWCNT. This phenomenon can be explained as follows: for a given torsional angle, the torque is proportional to D^3/L, where L is the tube length. When the inner and outer tubes in a DWCNT are long ($D \ll L$), they tend to twist together since their D^3/L are relatively less different from each other. However, for two tubes in a DWCNT of much shorter length, D^3/L for each tube become relatively different from each other, and the outer tube being subject to a much higher torque for a given torsional angle will buckle first.

In addition to the buckling behaviors of DWCNTs under torsion, the shear modules of DWCNTs are also calculated to investigate the length effect. Based on the relationship between torque and torsional angle $T = \frac{GJ}{L}\phi$, where J is the polar moment of inertia, ϕ the torsional angle, and the shear modulus G can be determined. For all DWCNTs with various lengths simulated herein, the shear modulus is found to lie in the range of 0.373–0.412 TPa by adopting the effective thickness of 3.4 Å for CNTs. The magnitudes of the shear modulus imply that the shear modulus of DWCNTs is relatively independent of length. Furthermore, the results are in good agreement with those given by others. For example, Lu [37] reported a shear modulus of 0.45 TPa by a force constant model. Hall *et al* [31] obtained a shear modulus of about 0.41 TPa in their torsional experiment. In the calculation of the shear modulus, Lu [37] and Hall *et al* [31] also assumed the thickness of CNTs as 3.4 Å.

4. Effect of the inner tube in DWCNTs

Recall that the presence of the inner tube leads to an enhancement of the torsional properties of DWCNTs resulting from the vdW interaction between the tubes. To further explore how the inner tube affects the torsional deformation of DWCNTs, MD simulations are conducted on the 114.5 Å-long DWCNT under two different conditions. The first MD simulation is performed on the DWCNT by twisting the outer tube only while the inner tube is free of rotation but the five rings of atoms are fixed at both ends. It is found that the outer tube reaches the critical torque at a torsional angle of 100°, the same as in the common case studied in the previous section (where the inner and outer tubes are rotated simultaneously). The critical torque obtained is 41.413 nN nm which is also close to 41.968 nN nm for the common case. The outer tube buckles under torsion and then drives the inner one to deform in the post-buckling stage.

In the second MD simulation on the same DWCNT, the simulation condition is kept identical to the first one except that the inner tube is totally free, i.e. not fixed to the end atoms. It is also found that the outer tube reaches the critical torque at the torsional angle of 100°. The magnitude of the critical torque is 41.291 nN nm which is also close to that of the common case. The post-buckling modes of the DWCNTs at the same torsional angle are displayed in figures 6(a)–(c) for the common and the foregoing two special cases, respectively. It is clearly seen from figures 6(b) and (c) that the deformed morphologies of DWCNTs with free or fixed inner tubes are rather similar, i.e. the inner tube deforms randomly due to the interaction from the outer tube. These deformed morphologies shown in figures 6(b) and (c) are distinct from figure 6(a) for the common case in which the inner and outer tubes are rotated simultaneously. The foregoing two special simulation cases imply that the introduction of the inner tube can enhance the torsional properties of the outer tube and the rate of enhancement is independent of the loading and boundary conditions of the inner tube. In other words, the torsional property of the outer tube in a DWCNT is insensitive to the loading and boundary conditions of its inner counterpart. In view of this, the experimental measurement of the torsional properties of MWCNTs may be done more easily since one does not need to pay attention to the loading and boundary conditions of the inner tubes.

The presence of the inner tube offer vdW interactions between the constituent tubes in DWCNTs. This vdW interaction makes the outer tube (and in the end, the whole DWCNT) stronger in resisting the external torque. This conclusion can be extended to MWCNTs. Recently, Huang *et al* [38] carried out coarse-grained simulations of a 10-walled MWCNT under torsion. Their simulation reveal that beyond the torsional bifurcation, the rippling pattern propagates from the outer to the inner layers, with the two innermost layers acting as a hard core that hardly ripples.

5. Conclusions

The torsional buckling behaviors of DWCNTs of various lengths are investigated by means of molecular dynamics simulations. Based on the simulation results, it is found that DWCNTs display gradual or simultaneous buckling modes depending on their lengths. For short DWCNTs under torsion, the outer tube buckles first followed by the inner one due to the relatively larger difference in their critical torques. The short DWCNT under torsion deforms progressively from the outer tube to the inner one, demonstrating a gradual buckling mode. For a slender DWCNT, the difference in the critical torques of the inner and outer tubes is relatively less. Thus the two tubes buckle almost simultaneously. The buckling behaviors of DWCNTs are sensitive to their lengths, but the shear modulus of DWCNTs is relatively independent of their lengths.

The presence of the inner tube in a DWCNT enhances the torsional property due to the stiffening effect produced by vdW interactions. It does not matter much if the inner tube is unrestrained at the ends or whether torque is applied to it, the enhanced torsional property is realized so long as the inner tube is present.

References

[1] Fennimore A M, Yuzvinsky T D, Han W Q, Fuhrer M S, Cumings J and Zettl A 2003 *Nature* **424** 408
[2] Williams P A, Papadakis S J, Patel A M, Falvo M R, Washburn S and Superfine R 2003 *Appl. Phys. Lett.* **82** 805
[3] Papadakis S J, Hall A R, Williams P A, Vicci L, Falvo M R, Superfine R and Washburn S 2004 *Phys. Rev. Lett.* **93** 146101
[4] Cornwell C F and Wille L T 1997 *Solid State Commun.* **101** 555–8
[5] Srivastava D, Menon M and Cho K 1999 *Phys. Rev. Lett.* **83** 2973
[6] Ni B, Sinnott S B, Mikulski P T and Harrison J A 2002 *Phys. Rev. Lett.* **88** 205505
[7] Buehler M J, Kong Y and Gao H J 2004 *J. Eng. Mater. Tech.* **126** 245
[8] Liew K M, Wong C H, He X Q, Tan M J and Meguid S A 2004 *Phys. Rev.* B **69** 115249
[9] Liew K M, Wong C H and Tan M J 2005 *Appl. Phys. Lett.* **87** 041901
[10] Chang T C, Li G Q and Guo W L 2005 *Carbon* **43** 287–94
[11] Chang T C, Guo W L and Guo X M 2005 *Phys. Rev.* B **72** 064101
[12] Liew K M, Wong C H and Tan M J 2006 *Acta Mater.* **54** 225–31
[13] Zhang Y Y, Wang C M and Tan V B C 2008 *J. Appl. Phys.* **103** 053505
[14] Falvo M R, Clary G J, Taylor R M, Chi V, Brooks F P Jr, Washburn S and Superfine R 1997 *Nature* **389** 582
[15] Huhtala M, Kuronen A and Kaski K 2001 *Mater. Res. Soc. Symp. Proc.* **706** 29.8
[16] Kutana A and Giapis K P 2006 *Phys. Rev. Lett.* **97** 245501
[17] Chang T C and Hou J 2006 *J. Appl. Phys.* **100** 114327
[18] Li X Y, Yang W and Liu B 2007 *Phys. Rev. Lett.* **98** 205502
[19] Duan X J, Tang C, Zhang J, Guo W L and Liu Z F 2007 *Nano Lett.* **7** 143–8
[20] Brenner D W 1990 *Phys. Rev.* B **42** 9458–71
[21] Yakobson B I, Brabec S J and Bernholc J 1996 *Phys. Rev. Lett.* **76** 2511–4
[22] Han Q and Lu G X 2003 *Eur. J. Mech.* A **22** 875–83
[23] Ru C Q 2001 *J. Mech. Phys. Solids* **49** 1265–79
[24] Yao X H and Han Q 2006 *J. Eng. Mater. Tech.* **128** 419
[25] Wang Q, Quek S T and Varadan V K 2007 *Phys. Lett.* A **367** 135–9
[26] Wang Y, Wang X X and Ni X G 2004 *Modelling Simul. Mater. Sci. Eng.* **12** 1099–107
[27] Chang T C 2007 *Appl. Phys. Lett.* **90** 201910
[28] Jeong B W, Lim J K and Sinnott S B 2007 *J. Appl. Phys.* **101** 084309
[29] Jeong B W, Lim J K and Sinnott S B 2008 *Appl. Phys. Lett.* **92** 253114
[30] Williams P A, Papadakis S J, Patel A M, Falvo M R, Washburn S and Superfine R 2002 *Phys. Rev. Lett.* **89** 255502
[31] Hall A R, An L, Liu J, Vicci L, Falvo M R, Superfine R and Washburn S 2006 *Phys. Rev. Lett.* **96** 256102
[32] Brenner D W, Shenderova O A, Harrison J A, Stuart S J, Ni B and Sinnott S B 2002 *J. Phys.: Condens. Matter* **14** 783–802
[33] Lennard-Jones J E 1924 *Proc. R. Soc.* A **106** 441–62
[34] Berendsen H J C, Postma J P M, van Gunsteren W F, Dinola A and Haak J R 1984 *J. Chem. Phys.* **81** 3684–90
[35] Zhang Y Y, Tan V B C and Wang C M 2007 *Carbon* **45** 514–23
[36] Wang Q 2008 *Carbon* **46** 1159–74
[37] Lu J P 1997 *Phys. Rev. Lett.* **79** 1297–300
[38] Huang X, Zou J and Zhang S L 2008 *Appl. Phys. Lett.* **93** 031915